

# Gas-Phase Formation of 1,3,5,7-Cyclooctatetraene ( $C_8H_8$ ) through Ring Expansion via the Aromatic 1,3,5-Cyclooctatrien-7-yl Radical ( $C_8H_9^\bullet$ ) Transient

Zhenghai Yang,<sup>§</sup> Galiya R. Galimova,<sup>§</sup> Chao He, Srinivas Doddipatla, Alexander M. Mebel,\* and Ralf I. Kaiser\*



Cite This: <https://doi.org/10.1021/jacs.2c06448>



Read Online

ACCESS |



Metrics & More

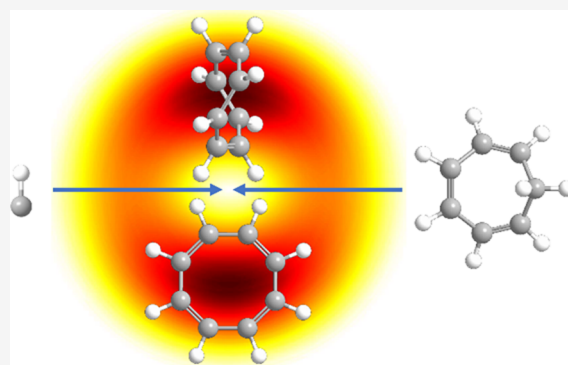


Article Recommendations



Supporting Information

**ABSTRACT:** Gas-phase 1,3,5,7-cyclooctatetraene ( $C_8H_8$ ) and triplet aromatic 1,3,5,7-cyclooctatetraene ( $C_8H_8$ ) were formed for the first time through bimolecular methylidyne radical ( $CH$ )–1,3,5-cycloheptatriene ( $C_7H_8$ ) reactions under single-collision conditions on a doublet surface. The reaction involves methylidyne radical addition to the olefinic  $\pi$  electron system of 1,3,5-cycloheptatriene followed by isomerization and ring expansion to an aromatic 1,3,5-cyclooctatrien-7-yl radical ( $C_8H_9^\bullet$ ). The chemically activated doublet radical intermediate undergoes unimolecular decomposition to 1,3,5,7-cyclooctatetraene. Substituted 1,3,5,7-cyclooctatetraene molecules can be prepared in the gas phase with hydrogen atom(s) in the 1,3,5-cycloheptatriene reactant being replaced by organic side groups. These findings are also of potential interest to organometallic chemists by expanding the synthesis of exotic transition-metal complexes incorporating substituted 1,3,5,7-cyclooctatetraene dianion ( $C_8H_8^{2-}$ ) ligands and to untangle the unimolecular decomposition of chemically activated and substituted 1,3,5-cyclooctatrien-7-yl radical, eventually gaining a fundamental insight of their bonding chemistry, electronic structures, and stabilities.



## 1. INTRODUCTION

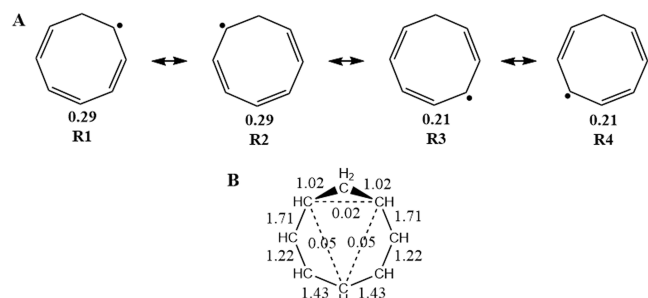
Ever since the preparation of 1,3,5,7-cyclooctatetraene (COT,  $C_8H_8$ ) from the alkaloid pseudopelletierine by Willstätter et al.<sup>1</sup> and through high-pressure tetramerization of acetylene ( $C_2H_2$ ) in the presence of nickelcyanide by Reppe et al.,<sup>2</sup> the COT molecule has received substantial interest from the preparative organometallic,<sup>3,4</sup> computational,<sup>5,6</sup> and physical-organic chemistry communities<sup>7,8</sup> from comprehensive insights of chemical bonding<sup>9</sup> and electronic structure.<sup>10</sup> Low-temperature  $^1H$  NMR studies<sup>11,12</sup> and X-ray diffraction data<sup>13,14</sup> revealed that COT adopts a  $D_{2d}$  symmetric tub conformation with two distinct carbon–carbon single (147 pm) and double (134 pm) bond distances.<sup>15</sup> These findings indicate that COT can be classified as a nonaromatic [8]annulene, i.e., a conjugated monocyclic hydrocarbon ( $C_nH_n$  with  $n$  being even) with alternating carbon–carbon single and double bonds. Singlet COT undergoes ring-inversion via a  $D_{4h}$  symmetric, planar transition state rather than via a  $D_{8h}$  symmetric transition state due to Jahn–Teller distortion.<sup>7,8</sup> This strongly contrasts the electronic structure of the  $10\pi$  Hückel aromatic,  $D_{8h}$  symmetric 1,3,5,7-cyclooctatetraene dianion ( $C_8H_8^{2-}$ ), a prevalent ligand in actinide sandwich coordination complexes such as thorocene ( $Th(C_8H_8)_2$ ) and uranocene ( $U(C_8H_8)_2$ ) as potential contenders for single molecular magnets<sup>16,17</sup> and nanowires.<sup>18,19</sup>

Nevertheless, despite the very first synthesis of COT more than a century ago, the 1,3,5-cyclooctatrien-7-yl radical ( $C_8H_9^\bullet$ ), which can be formed from COT by adding an atomic hydrogen to one of the four carbon–carbon double bonds, has not been inferred in any gas-phase experiments to date. Lin et al.<sup>20</sup> advocated that this radical may signify a hitherto overlooked transient hydrocarbon in combustion processes accessed through the phenyl radical ( $C_6H_5$ )–ethylene ( $C_2H_4$ ) reaction, possibly via the phenyl radical addition to ethylene followed by isomerization to a bicyclic complex and ring opening to the 1,3,5-cyclooctatrien-7-yl radical. Heat of formation at 0 K of  $325 \text{ kJ mol}^{-1}$  suggested by electronic structure calculations reveals that the 1,3,5-cyclooctatrien-7-yl radical is thermodynamically less stable than the *o*-, *m*-, and *p*-xylyl ( $CH_3C_6H_4CH_2^\bullet$ ) structural isomers by  $144\text{--}158 \text{ kJ mol}^{-1}$ .<sup>21–23</sup> Characteristically, 1,3,5-cyclooctatrien-7-yl represents a resonantly stabilized free radical

Received: June 19, 2022

(RSFR), which can be visualized through four nonequivalent resonance structures (Scheme 1), in which the spin density of

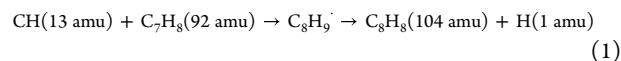
**Scheme 1. Four Nonequivalent Resonance Structures (R1–R4) along with the Corresponding Population (A) and the Natural Bond Orbital (NBO)–Computed Bond Orders (Wiberg Bond Indices) (B) of 1,3,5-Cyclooctatrien-7-yl ( $C_8H_9^\bullet$ , iS)**



the radical center transfers through the ring from C2 (R1) via C4 (R2) and C6 (R3) to C8 (R4). The radical center location directs the chemistry of molecular mass growth processes through radical–radical reactions or degradation via recombination with molecular oxygen followed by oxidation; hence, bimolecular gas-phase reactions of  $C_8H_9^\bullet$  may tetrafurcate through distinct barrierless addition intermediates represented through the radical centers in R1–R4.

Herein, an exceptional glimpse is afforded into the previously overlooked chemistry of the 1,3,5-cyclooctatrien-7-yl ( $C_8H_9^\bullet$ ) transient accessed in a bimolecular methylidyne radical (CH)–1,3,5-cycloheptatriene ( $C_7H_8$ ) reaction under single-collision conditions via ring expansion (reaction [1])

(Experimental Section). Under single-collision conditions, 1,3,5-cyclooctatrien-7-yl undergoes predominantly unimolecular decomposition to 1,3,5,7-cyclooctatetraene ( $C_8H_8$ , COT) plus atomic hydrogen thus providing an unconventional, previously elusive route to COT via a resonantly stabilized, chemically activated, and partially aromatic 1,3,5-cyclooctatrien-7-yl radical intermediate in combustion systems. This reaction is also stimulating from the viewpoint of physical-organic chemistry community acting as a prototype in the elucidation of the chemical reactivity, isomerization pathways, bond rupture processes, and the preparation of resonantly stabilized free-radical (RSFR) intermediates along with a highly unsaturated, cyclic molecule (COT), which cannot be explored by traditional synthetic routes



## 2. RESULTS

**2.1. Laboratory Frame.** In the methylidyne radical (CH,  $X^2\Pi$ ; 13 amu)–1,3,5-cycloheptatriene ( $C_7H_8$ ,  $X^1A'$ ; 92 amu) reaction, scattering signals could be detected at mass-to-charge ( $m/z$ ) ratios of 104 ( $C_8H_8^+ / ^{13}C_7H_7^+$ ) and 103 ( $C_8H_7^+ / ^{13}CC_7H_6^+$ ). After scaling, the time-of-flight (TOF) spectra at 104 and 103 were found to be superimposable, suggesting that the signal at  $m/z$  103 originates from dissociative ionization of the parent at  $m/z = 104$ . Figure 1 displays representative TOF spectra collected at different angles at 103. The corresponding laboratory angular distribution (LAD) is extracted by integrating the TOF spectra. This distribution reveals a maximum around  $59.5 \pm 0.3^\circ$  [center-of-mass (CM) angle] and is spread over  $25^\circ$  within the scattering plane (Table S1), which indicate indirect

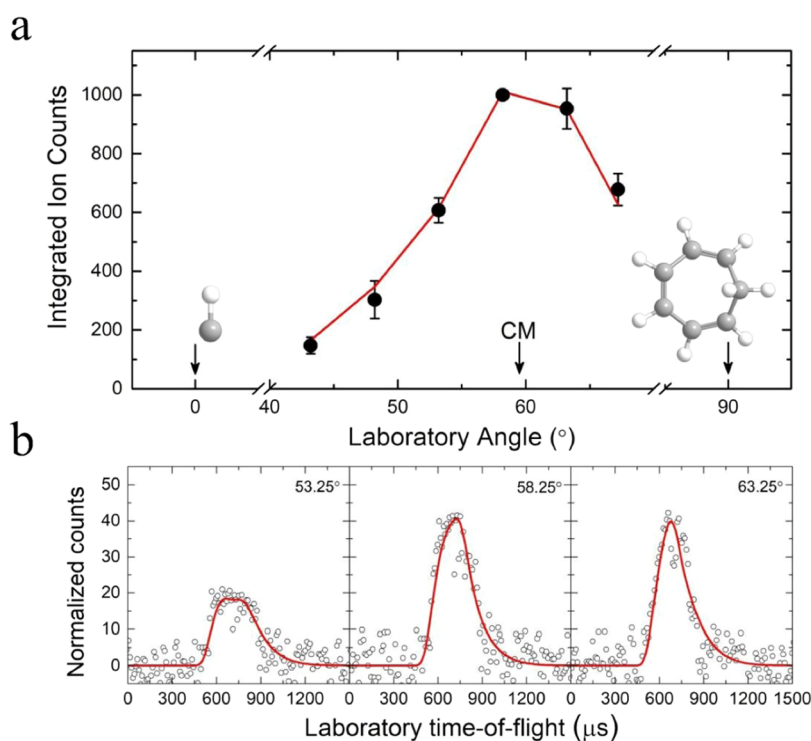


**Figure 1.** Laboratory angular distribution (LAD) (a) and selected TOF spectra (b) recorded at  $m/z$  of 103 ( $C_8H_7^+$ ). The open and solid circles define the experimental data, and the solid red lines indicate the best fits. Carbon and hydrogen atoms are color-coded in gray and white, respectively.

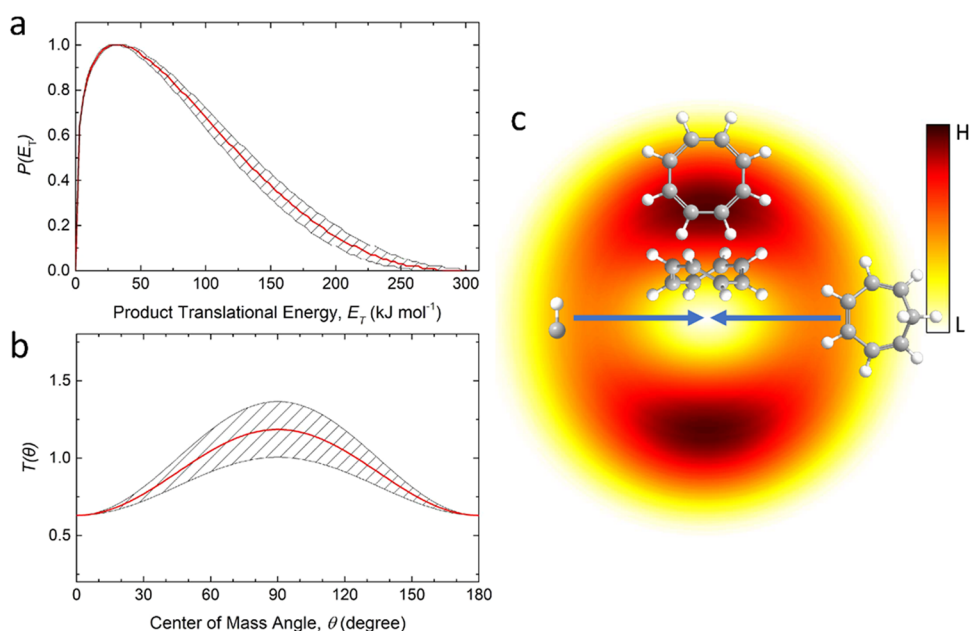
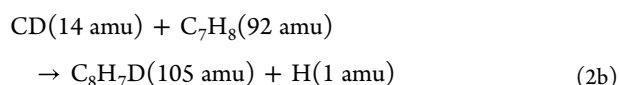
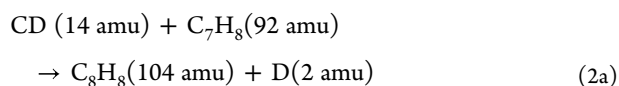


**Figure 2.** CM translational energy (a), angular flux distributions (b), and the flux contour map (c). The solid red lines and shaded areas define the best fit and the error limits, respectively.

scattering dynamics<sup>24</sup> and the existence of chemically activated  $C_8H_9$  complexes decomposing through atomic hydrogen loss to  $C_8H_8$  isomer(s).<sup>25,26</sup> Therefore, our raw data alone reveal the methylidyne versus hydrogen atom exchange pathway to  $C_8H_8$  isomer(s) (reaction [1]). Recall that the QMS is operated in the TOF mode, recording the flight time from the interaction region to the detector of a selected, well-defined  $m/z$  (Figure 1); this instrument does not collect a traditional mass spectrum of an organic compound as available from, e.g., the NIST database.<sup>27</sup>

Since the atomic hydrogen can be eliminated from the methylidyne and/or 1,3,5-cycloheptatriene reactant(s), we also conducted a crossed beam experiment of D1-methylidyne (CD, X<sup>2</sup>Π; 14 amu) with 1,3,5-cycloheptatriene and collected signals at 105 and 104; note that for this system, a signal at 104 can also form the  $C_8H_7D$  parent via dissociative electron-impact ionization. Our experiments revealed signals at 105 and 104 at a ratio of  $(0.46 \pm 0.03):1$  (Figure S1). However, since the branching ratio of the ion counts for ionization of the  $C_8H_8$  product ( $m/z = 104$ ) versus the ion counts from dissociative ionization ( $m/z = 103$ ) was determined to be  $(0.44 \pm 0.03):1$  for reaction [1], the contributions of dissociative electron-impact ionization from  $C_8H_7D$  (reaction [2b]) and reactive scattering signal forming  $C_8H_8$  (reaction [2a]) can be untangled. Within the error limits, the branching ratios for CH/ $C_7H_8$  and CD/ $C_7H_8$  systems are identical, revealing that the atomic hydrogen is ejected from the 1,3,5-cycloheptatriene reactant



**2.2. Center-of-Mass Frame.** With the identification of the  $C_8H_8$  product prepared via the H loss pathway, we are moving

on to the nature of the  $C_8H_8$  isomer(s) and the underlying formation mechanisms.<sup>28</sup> This is accomplished by converting the laboratory data (TOF, LAD) into the CM reference frame. This procedure effectively yields  $P(E_T)$  and  $T(\theta)$  distributions as shown in Figure 2.

Best fits could be accomplished by reproducing the laboratory data with a single reaction channel (product masses: 104 amu ( $C_8H_8$ ) plus 1 amu (H)). The  $P(E_T)$  prolongs to a maximum ( $E_{\text{max}}$ ) release of  $278 \pm 19 \text{ kJ mol}^{-1}$ , which can be utilized to compute the energy of reaction [1] and to identify the product(s) formed in the bimolecular reaction. Considering energy conservation and the lack of excitation in the reaction,  $E_{\text{max}}$  resembles the collision energy ( $20.8 \text{ kJ mol}^{-1}$ ) plus the reaction exoergicity. Consequently, this relationship leads to a reaction exoergicity of  $257 \pm 19 \text{ kJ mol}^{-1}$ . In addition, a distribution maximum of close to  $30 \text{ kJ mol}^{-1}$  of  $P(E_T)$  is depicted, suggesting a tight exit transition state associated with an extensive reorganization of the electron density upon unimolecular decomposition of the  $C_8H_9$  complex(es) to  $C_8H_8$  (104 amu) plus H (1 amu) products. Furthermore, the forward-backward symmetric  $T(\theta)$  indicates that the reaction proceeds through indirect scattering dynamics via the involvement of  $C_8H_9$  complex(es) with lifetime(s) longer than the rotational period.<sup>24</sup> The distribution maximum at  $90^\circ$  strongly infers geometrical constraints upon decomposition of the  $C_8H_9$  intermediate with an emission of the atomic hydrogen nearly perpendicularly to the plane spanned through the rotation of the molecule.<sup>29</sup> This finding is also supported by the flux contour map, which shows an overall image of the reaction and the scattering process.

### 3. DISCUSSION

The nature of the  $C_8H_8$  isomer is now identified through a comparison of the experimentally derived exoergicity of  $257 \pm 19 \text{ kJ mol}^{-1}$  with those reaction energies extracted from calculations. The geometries of  $C_8H_8$  isomers together with  $C_8H_9$  intermediates were explored through electronic structure calculations at an accuracy of  $\pm 8 \text{ kJ mol}^{-1}$ ; statistical

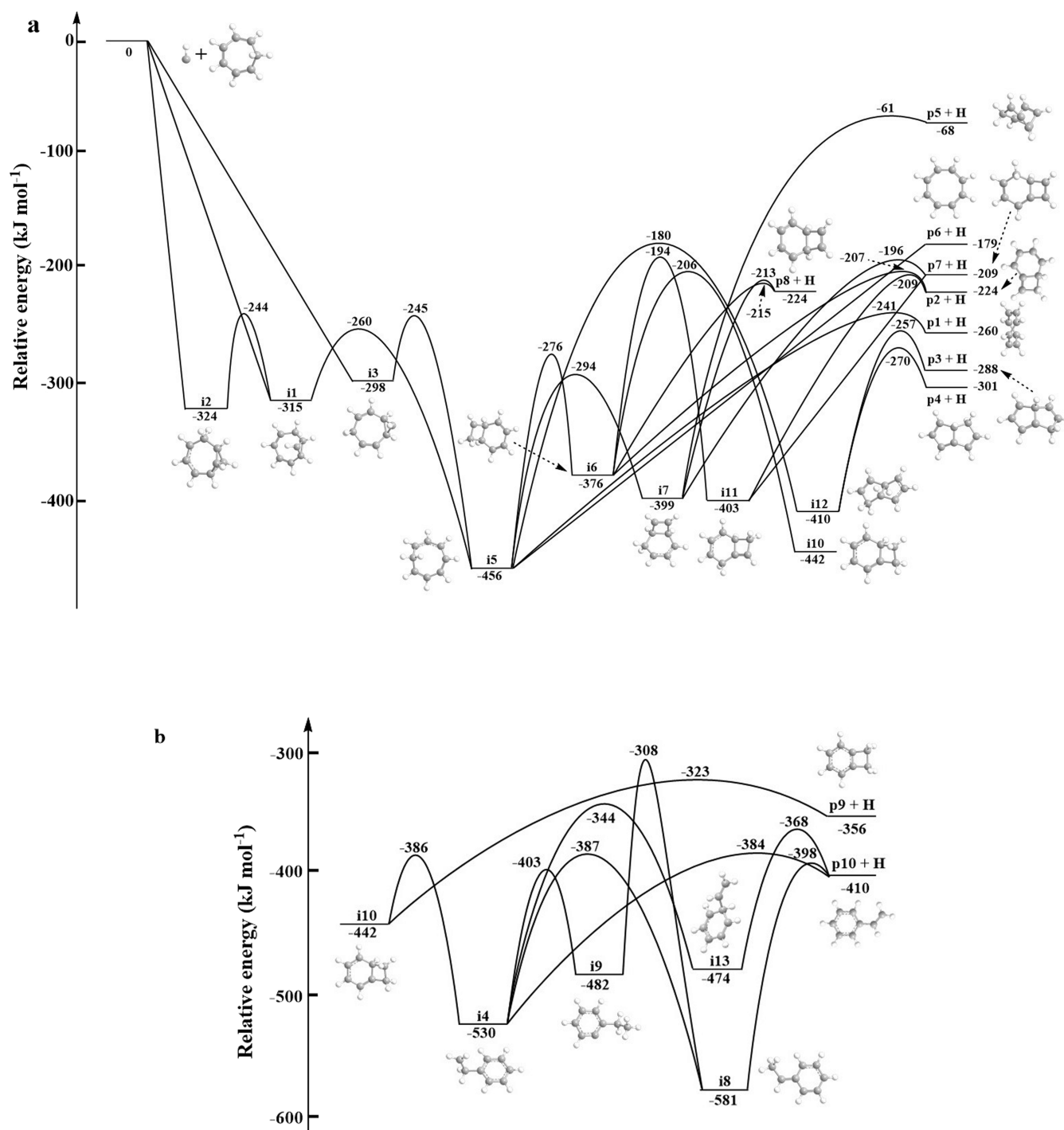


**Figure 3.** Potential energy surface (PES) for the reaction of methylidyne with 1,3,5-cycloheptatriene (a) and reaction pathways starting with **i10** leading to **p9** and **p10** (b).

calculations exploiting Rice–Ramsperger–Kassel–Marcus (RRKM) theory were also conducted (Figures 3, S3, Tables S2, and S3).<sup>30,31</sup> This study revealed the existence of multiple exit channels forming 10 distinct  $C_8H_8$  isomers (**p1**–**p10**) with overall reaction exoergicities between 68 and 410  $\text{kJ mol}^{-1}$ . These 10 isomers can be arranged in four groups with (i) one eight-membered ring (**p1**, **p6**), (ii) a fused six- and four-membered ring (**p2**, **p5**, **p7**, **p8**, **p9**), (iii) two fused five-membered rings (**p3**, **p4**), and (iv) a six-membered ring connected to a vinyl group (**p10**). Recall that the results from the CD/ $C_7H_8$  system revealed an exclusive hydrogen loss from

the closed shell hydrocarbon reactant, but no atomic deuterium elimination from the D1-methylidyne radical. This finding can be applied to eliminate **p2**, **p5**, **p7**, and **p10** as possible products. Here, the channels to these products would involve hydrogen *and* deuterium losses (Figure S4); since deuterium elimination has not been observed experimentally, these products can be discounted. With the elimination of **p2**, **p5**, **p7**, and **p10**, we now compare the experimental reaction exoergicities of  $257 \pm 19 \text{ kJ mol}^{-1}$  with computed reaction energies of the remaining product isomers (Figure 3). An analysis of the experimental reaction energy and the computed

energetics suggests that 1,3,5,7-cyclooctatetraene (**p1**,  $C_8H_8$ , COT) well matches the experimental values ( $-257 \pm 19$   $\text{kJ mol}^{-1}$ ) with the computed values ( $-260 \pm 8$   $\text{kJ mol}^{-1}$ ). A detail inspection of the potential energy surface (PES) reveals that unimolecular decomposition of chemically activated **i5** can lead to 1,3,5,7-cyclooctatetraene (**p1**) through atomic hydrogen loss involving a tight exit transition state located 19  $\text{kJ mol}^{-1}$  above the separate reactants. The geometries of the exit transition state forming **p1** reveal that the atomic hydrogen is emitted nearly perpendicular ( $61.7^\circ$ ; Figure 4) to the plane of

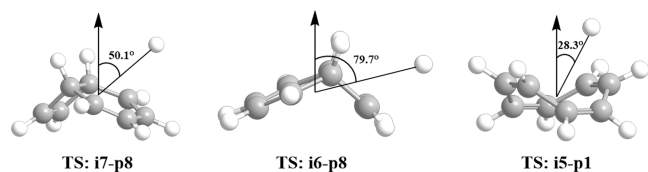


**Figure 4.** Computed geometries of the exit transition states leading to **p1** and **p8**.

the rotating complex, agreeing with the sideways scattering fitting of the  $T(\theta)$  distributions. Overall, the bimolecular reaction is initiated through barrierless addition of methylidyne to one of the carbon–carbon double bonds forming bicyclic reaction intermediates **i1**, **i2**, and/or **i3**, which eventually isomerize to **i5** via the opening of the annulated three-membered ring moiety to the eight-membered ring structure.

The electronic structure and chemical bonding of **i5** are peculiar. The natural bond orbital population analysis (NBO) reveals that bond delocalization in **i5** is described through four resonance structures contributing about 30% (**R1**, **R2**) and 20% (**R3**, **R4**) (Scheme 1). This intermediate is nonplanar but possesses  $C_s$  symmetry along with the  $X^2A'$  ground electronic state. A  $C_{2v}$  stationary point (TS), in which all eight carbon atoms are in one plane, is 36  $\text{kJ mol}^{-1}$  higher in energy than **i5** and represents an inversion transition state; no local minimum exists with seven CH moieties in the same plane and the remaining  $\text{CH}_2$  group out of plane. This inversion barrier is much lower than that in the cyclooctatrienyl cation ( $C_8H_9^+$ ), i.e., 93  $\text{kJ mol}^{-1}$ .<sup>29</sup> The lower isomerization barrier would essentially result in a floppy intermediate **i5** in which all carbon atoms are in one plane, hence resulting in a hydrogen atom elimination nearly perpendicular to the rotating plane of the decomposing intermediate.

Note that an assignment of the  $C_{2v}$  symmetric transition state as homoaromatic within a Hückel-like model is not feasible. Homoaromatic molecules are classified as organic compounds that show aromatic characters even though the molecular conjugation is interrupted by a  $\text{CH}_2$  moiety. The  $C_{2v}$  structure of the cyclooctatrienyl cation ( $C_8H_9^+$ ) was assigned as  $8\pi$  antiaromatic, considering that the  $\text{CH}_2$  bridge provides two pseudo  $\pi$  electrons into the  $\pi$  system, whereas the  $C_{2v}$  structure of the cyclooctatrienyl anion ( $C_8H_9^-$ ) is  $10\pi$  aromatic.<sup>32</sup> However, in the  $C_8H_9$  radical **i5**, we have  $9\pi$  electrons, which is an intermediate case (Figure 5). Likewise, the nonplanar structure of the cyclooctatrienyl cation ( $C_8H_9^+$ ) can be assigned as  $8\pi$  Möbius aromatic.<sup>33</sup> However, this term is not appropriate for the  $C_8H_9$  radical **i5**, since formally there are  $9\pi$  electrons in the radical. Nevertheless, ring delocalization in **i5** is clearly present as it is evidenced by the NBO-computed bond orders (Wiberg bond indices), which show some  $\pi$ -character for all C–C bonds, even for the  $\text{CH–CH}_2\text{–CH}$

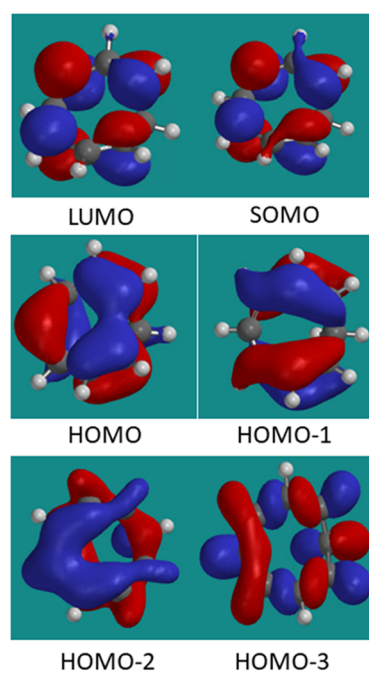
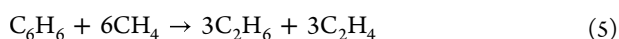
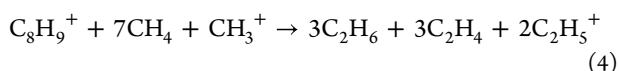
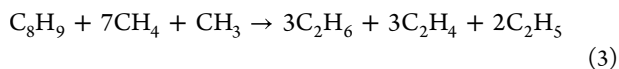


**Figure 5.** Molecular orbitals of 1,3,5-cyclooctatrien-7-yl radical ( $C_8H_9^\bullet$ ) **i5**.

moiety and nonzero values across the ring (Scheme 1 and Figure 3). Also, the molecular orbital picture (Figure 5) shows that the three highest doubly occupied molecular orbitals (HOMO, HOMO – 1, and HOMO – 2) exhibit a clear  $\pi$ -bonding character typical for an aromatic ring system and with participation of the  $\text{CH}_2$  group in HOMO and HOMO – 2, whereas HOMO – 3 represents an ensemble of  $\sigma$  bonds. Alternatively, the singly occupied and lowest unoccupied molecular orbitals (SOMO and LUMO) display a typical  $\pi^*$ -antibonding character.

Aromaticity of a molecule is usually considered in terms of three criteria, structural, energetic, and magnetic.<sup>34</sup> The nonplanar  $C_s$ -symmetric structure of cyclooctatrienyl cation has been assigned as strongly aromatic<sup>35</sup> and hence, here, we assess the aromaticity of  $C_8H_9i5$  by comparing the three criteria in the radical and the cation. Structurally, the C–C bond alteration (in Å, as optimized at the B3LYP/6-311 G(d,p) level) in the radical (1.507, 1.353, 1.433, and 1.399) is similar but somewhat higher than that in the cation (1.490, 1.377, 1.403, and 1.399). The aromatic stabilization energy for **i5** computed using the isodesmic reaction [3] is 219  $\text{kJ mol}^{-1}$ . This is close to the stabilization energy of the corresponding cyclooctatrienyl cation ( $C_8H_9^+$ ) of 230  $\text{kJ mol}^{-1}$  computed earlier via equation [4].<sup>33</sup> Therefore, compared to the aromatic ring stabilization energy for benzene (equation [5]) of 274  $\text{kJ mol}^{-1}$ , both the cation and **i5** have to be classified as less aromatic. Interestingly, the energetic stabilization of the cation and the  $C_8H_9i5$  radical can be partially explained in terms of double hyperconjugation, as for antiaromatic singlet  $D_{2d}$ -symmetric COT,<sup>36</sup> in addition to the  $\pi$  bond conjugation. Although the structures of both  $C_8H_9^+$  and **i5** are less puckered/twisted than that of COT, the CCCC dihedral angles for the seven C atoms in  $C_8H_9^+$  and **i5** taking part in C–C bonds with a delocalized  $\pi$  component are in the  $11\text{--}32^\circ$  range compared to  $56^\circ$  in COT. According to the NBO analysis by Schleyer and co-workers,<sup>36</sup> both  $\pi$  bond conjugation and double hyperconjugation contribute to the

enhancement of bonding at these angles. Finally, we explored magnetic properties of the radical using the nuclear independent chemical shift (NICS)<sup>37</sup> scan method.<sup>38,39</sup> It is known that the out-of-plane component of the magnetic shielding tensor, NICS<sub>ZZ</sub>, displays a profound minimum at 0 Å in aromatic molecules, has a maximum in antiaromatic species, and has a shallow minimum in nonaromatic compounds.<sup>35,37</sup> As seen in Figure S7, NICS<sub>ZZ</sub> of **i5** displays a deep minimum at 0 Å, with the lowest value of −16.5 ppm. The minimum is not as deep as that for the cation, −31.7 ppm, and considering all three criteria of aromaticity together, we conclude that C<sub>8</sub>H<sub>9</sub>**i5** is aromatic, though less aromatic than the nonplanar C<sub>8</sub>H<sub>9</sub><sup>+</sup> cyclooctatrienyl cation



The identification of the 1,3,5-cyclooctatrien-7-yl radical (C<sub>8</sub>H<sub>9</sub><sup>•</sup>) **i5** as the decomposing intermediate along with the analysis of alternative decomposition pathways of **i5** suggests that the formation of 1,3,5,7-cyclooctatetraene (**p1**, C<sub>8</sub>H<sub>8</sub>) is preferred. Formation of the thermodynamically preferred products **p3** and **p4** requires hydrogen elimination from **i12**, which can only be accessed via isomerization through ring closure of **i5** involving a barrier of 270 kJ mol<sup>−1</sup>. This pathway is clearly unfavorable compared to the **i5** → **p1** + H channel with a transition state 61 kJ mol<sup>−1</sup> below the transition state for **i5** → **i12**. Analogous arguments such as the energy of the transition states compared to the **i5** → **p1** + H channel render the formation of **p2**, **p7**, and **p8** less likely, leaving only the barrierless decomposition **i5** → **p6** (triplet aromatic 1,3,5,7-cyclooctatetraene, a<sup>3</sup>A<sub>1g</sub>) + H slightly competitive. These conclusions are also corroborated by statistical RRKM calculations (Table S2). Here, from **i5**, 1,3,5,7-cyclooctatetraene (**p1**) and triplet aromatic 1,3,5,7-cyclooctatetraene (**p6**) dominate the overall product yields with nearly 80% with a branching ratio of **p1**–**p6** of about 4.

## 4. CONCLUSIONS

To sum up, our combined computational and experimental study of the bimolecular gas-phase reaction of the simplest organic radical-methylidyne radical (CH) with 1,3,5-cycloheptatriene (C<sub>7</sub>H<sub>8</sub>) revealed a facile and barrierless gas-phase preparation of 1,3,5,7-cyclooctatetraene (C<sub>8</sub>H<sub>8</sub>) and triplet aromatic 1,3,5,7-cyclooctatetraene (C<sub>8</sub>H<sub>8</sub>) under single-collision conditions. The formation route involves addition of the methylidyne radical to the olefinic π electron system of 1,3,5-cycloheptatriene (C<sub>7</sub>H<sub>8</sub>) followed by isomerization of the collision complexes and ring expansion to the aromatic 1,3,5-cyclooctatrien-7-yl radical (C<sub>8</sub>H<sub>9</sub><sup>•</sup>) **i5**. McIntosh et al.<sup>40</sup> proposed the existence of matrix-isolated 1,3,5-cyclooctatrien-7-yl upon <sup>60</sup>Co γ-irradiated 1,3,5,7-cyclooctatetraene (C<sub>8</sub>H<sub>8</sub>) based on electron spin resonance (ESR) and intermediate neglect of differential overlap (INDO) calculations. This matrix isolation study was verified by Korth et al.<sup>41</sup> through a radiation-induced carbon–hydrogen bond rupture from the methylene (CH<sub>2</sub>) moiety within the seven-membered ring in bicyclo[5.1.0]octa-2,5-diene, followed by ring opening of the doublet radical to the 1,3,5-cyclooctatrien-7-yl radical via a

barrier of about 100 kJ mol<sup>−1</sup>. The barrierless gas-phase preparation of 1,3,5,7-cyclooctatetraene (C<sub>8</sub>H<sub>8</sub>) and triplet aromatic 1,3,5,7-cyclooctatetraene (C<sub>8</sub>H<sub>8</sub>) accesses exotic and aromatic doublet radical intermediates such as the 1,3,5-cyclooctatrien-7-yl radical on the doublet surface, which cannot be synthesized through classical synthetic chemistry protocols. Further, substituted 1,3,5,7-cyclooctatetraene molecules can be prepared in the gas phase with hydrogen atom(s) in the 1,3,5-cycloheptatriene (C<sub>7</sub>H<sub>8</sub>) reactant being replaced by organic side groups. Therefore, prospective crossed molecular beam and theoretical studies of exotic, substituted doublet radical intermediates and singlet/triplet 1,3,5,7-cyclooctatetraene are clearly endorsed to systematically unravel the unimolecular decomposition of aromatic doublet radical intermediates to afford a comprehensive knowledge of their unimolecular decomposition dynamics along with bonding chemistry, electronic structures, and stabilities.

## 5. EXPERIMENTAL AND COMPUTATIONAL SECTION

**5.1. Experimental Section.** The gas-phase reaction of methylidyne (CH, X<sup>2</sup>Π) with 1,3,5-cycloheptatriene (C<sub>7</sub>H<sub>8</sub>, X<sup>1</sup>A') was performed in a crossed molecular beam machine.<sup>28,42</sup> The supersonic beam of methylidyne was generated through photodissociation (COMPex 110; 248 nm; 30 Hz) of bromoform (CHBr<sub>3</sub>; Aldrich; ≥99%; 283 K; helium-seeded; 2.2 atm).<sup>43</sup> After the skimmer and chopper wheel, the selected CH beam was defined with a *v<sub>p</sub>* (peak velocity) of 1857 ± 19 m s<sup>−1</sup> and a *S* (speed ratio) of 13.2 ± 0.6 (Table S1). Using laser-induced fluorescence, the rotational temperature of 14 ± 1 K of the CH radical beam was determined.<sup>44,45</sup> The supersonic beam of 1,3,5-cycloheptatriene (TCI) seeded in krypton (Praxair, 99.999%) was released by a second piezoelectric pulse valve (550 Torr; *v<sub>p</sub>*: 445 ± 7 m s<sup>−1</sup>; *S*: 15.0 ± 0.2). Bromoform-d was also used as a precursor yielding a D1-methylidyne beam (*v<sub>p</sub>*: 1845 ± 21 m s<sup>−1</sup>; *S*: 13.5 ± 0.8). Both primary and secondary reactants were held in a stainless steel bubbler. The primary beam crossed the C<sub>7</sub>H<sub>8</sub> beam perpendicularly, leading to a collision energy of 20.8 ± 0.4 kJ mol<sup>−1</sup> and a Θ<sub>CM</sub> of 59.5 ± 0.3° (Table S1). The whole detector is rotatable to collect the TOF spectra at desired angles. After electron-impact ionization,<sup>46</sup> the products were monitored using a QMS (Extrel, QC 150) and a Daly-type ion counter<sup>47</sup> under ultrahigh-vacuum conditions (7 × 10<sup>−12</sup> Torr). A forward convolution method was employed to fit the data and *P*(*E<sub>T</sub>*), the *T*(θ) flux distributions and the contour flux map, *I*(*u*, θ) ≈ *P*(*u*) × *T*(θ), with the CM velocity *u* and angle θ are provided. The *T*(θ) and *P*(*E<sub>T</sub>*) flux distributions are varied iteratively until a best fit of the laboratory TOF spectra and angular distribution is obtained.<sup>24</sup>

**5.2. Computational Section.** Geometric structures of various species (CH and C<sub>7</sub>H<sub>8</sub>, different products, C<sub>8</sub>H<sub>9</sub> intermediates, and transition states) on the PES accessed by the reaction of the methylidyne radical with 1,3,5-cycloheptatriene were optimized at the hybrid DFT B3LYP level with the 6-311G(d,p) basis set.<sup>48,49</sup> Vibrational frequency calculations were carried out using the same B3LYP/6-311G(d,p) method. Single-point energies were further refined using the G3(MP2,CC)//B3LYP/6-311G(d,p) variant of the G3 model chemistry scheme.<sup>50–52</sup> The anticipated accuracy of the composite approach relative energies is typically within 5–10 kJ mol<sup>−1</sup> or better. This estimate of accuracy is based on average absolute deviations from the experiment of calculated enthalpies of formation, ionization energies, and electron and proton affinities of various molecules and radicals,<sup>52</sup> as well as on the vast experience of this group in applications of the G3 model chemistry schemes to the studies of PESs and kinetics of chemical reactions involving hydrocarbons in singlet, doublet, and triplet electronic states in the last two decades. The GIAO method using B3LYP/6-311++G(d,p) for electronic structure calculations was employed to evaluate NICS values.<sup>53,54</sup> The GAUSSIAN 09<sup>55</sup> and MOLPRO 2010<sup>56</sup> software packages were utilized for ab initio calculations. For unimolecular

reaction steps on the C<sub>8</sub>H<sub>8</sub> PES, which follow initial association of CH with 1,3,5-cycloheptatriene, rate constants were assessed within the framework of the Rice–Ramsperger–Kassel–Marcus (RRKM) theory.<sup>57–59</sup> For the i5 → p6 + H decomposition channel occurring without an exit barrier, microcanonical variational RRKM theory was employed where the minimal energy path (MEP) and molecular properties of the structures along the MEP were also computed at the G3(MP2,CC)//B3LYP/6-311G(d,p) level. In the the RRKM calculations of energy-dependent rate constants, the internal energy of each species (intermediate or transition state) was assumed to be equal to the sum of the collision energy and the energy of chemical activation, which in turn equates to a negative of the relative energy of the species with regard to the CH + C<sub>7</sub>H<sub>8</sub> reactants. The zero-pressure approach is validated by the fact that the reacting C<sub>8</sub>H<sub>8</sub> intermediates in crossed molecular beams cannot undergo any collisional activation/deactivation. Next, first-order kinetic equations were solved in a steady-state approximation<sup>60</sup> using the computed RRKM rate constants and employing our own Unimol code to obtain product branching ratios under single-collision conditions.<sup>61</sup>

## ■ ASSOCIATED CONTENT

### SI Supporting Information

The Supporting Information is available free of charge at <https://pubs.acs.org/doi/10.1021/jacs.2c06448>.

Experimental parameters (Table S1), statistical branching ratios at the collision energies of 0 and 20 kJ mol<sup>-1</sup> (Table S2), optimized coordinates and calculated vibrational frequencies for stationary structures involved in the CH–C<sub>7</sub>H<sub>8</sub> reaction (Table S3); CM TOF spectra of CH–C<sub>7</sub>H<sub>8</sub> and CD–C<sub>7</sub>H<sub>8</sub> reactions (Figure S1), molecular structures of p1 and p6 (Figure S2), complete PES (Figure S3), the atomic hydrogen or deuterium loss channels in the CD–C<sub>7</sub>H<sub>8</sub> reaction (Figure S4), 2D and 3D structures of the products (Figure S5) and intermediates (Figure S6), and GIAO-B3LYP/6-311G+(d,p)-calculated NICS values at various positions along the z-axis (Figure S7) (PDF)

## ■ AUTHOR INFORMATION

### Corresponding Authors

Alexander M. Mebel – Department of Chemistry and Biochemistry, Florida International University, Miami, Florida 33199, United States; [orcid.org/0000-0002-7233-3133](https://orcid.org/0000-0002-7233-3133); Email: [mebela@fiu.edu](mailto:mebela@fiu.edu)

Ralf I. Kaiser – Department of Chemistry, University of Hawai'i at Manoa, Honolulu, Hawaii 96822, United States; [orcid.org/0000-0002-7233-7206](https://orcid.org/0000-0002-7233-7206); Email: [ralfk@hawaii.edu](mailto:ralfk@hawaii.edu)

### Authors

Zhenghai Yang – Department of Chemistry, University of Hawai'i at Manoa, Honolulu, Hawaii 96822, United States

Galiya R. Galimova – Department of Chemistry and Biochemistry, Florida International University, Miami, Florida 33199, United States

Chao He – Department of Chemistry, University of Hawai'i at Manoa, Honolulu, Hawaii 96822, United States

Srinivas Doddipatla – Department of Chemistry, University of Hawai'i at Manoa, Honolulu, Hawaii 96822, United States

Complete contact information is available at:

<https://pubs.acs.org/doi/10.1021/jacs.2c06448>

### Author Contributions

<sup>§</sup>Z.Y. and G.R.G. contributed equally to this work.

## Notes

The authors declare no competing financial interest.

## ■ ACKNOWLEDGMENTS

This work was supported by the U.S. Department of Energy, Basic Energy Sciences, by Grant No. DE-FG02-03ER15411 to the University of Hawaii at Manoa and No. DE-FG02-04ER15570 to the Florida International University.

## ■ REFERENCES

- (1) Willstätter, R.; Waser, E. Über Cyclo-octatetraen. *Ber. Dtsch. Chem. Ges.* **1911**, *44*, 3423–3445.
- (2) Reppe, W.; Schlichting, O.; Klager, K.; Toepel, T. Cyclisierende Polymerisation von Acetylen I Über Cyclooctatetraen. *Justus Liebigs Ann. Chem.* **1948**, *560*, 1–92.
- (3) Murahashi, T.; Kato, N.; Ogoshi, S.; Kurosawa, H. Synthesis and Structure of Dipalladium Complexes Containing Cyclooctatetraene and Bicyclooctatrienyl Ligands. *J. Organomet. Chem.* **2008**, *693*, 894–898.
- (4) Sroor, F. M. Recent Progress of Organometallic Cyclooctatetraenide Dianion Chemistry. *J. Organomet. Chem.* **2021**, *948*, No. 121878.
- (5) Frutos, L. M.; Castano, O.; Andrés, J. L.; Merchán, M.; Acuna, A. U. A Theory of Nonvertical Triplet Energy Transfer in terms of Accurate Potential Energy Surfaces: The Transfer Reaction from  $\pi$ ,  $\pi^*$  Triplet Donors to 1, 3, 5, 7-Cyclooctatetraene. *J. Chem. Phys.* **2004**, *120*, 1208–1216.
- (6) Hrovat, D. A.; Borden, W. T. CASSCF Calculations Find That a D<sub>8h</sub> Geometry Is the Transition State for Double Bond Shifting in Cyclooctatetraene. *J. Am. Chem. Soc.* **1992**, *114*, 5879–5881.
- (7) Klärner, F. G. About the Antiaromaticity of Planar Cyclooctatetraene. *Angew. Chem., Int. Ed.* **2001**, *40*, 3977–3981.
- (8) Wenthold, P. G.; Hrovat, D. A.; Borden, W. T.; Lineberger, W. C. Transition-State Spectroscopy of Cyclooctatetraene. *Science* **1996**, *272*, 1456–1459.
- (9) Garavelli, M.; Bernardi, F.; Cembran, A.; Castano, O.; Frutos, L. M.; Merchán, M.; Olivucci, M. Cyclooctatetraene Computational Photo- and Thermal Chemistry: A Reactivity Model for Conjugated Hydrocarbons. *J. Am. Chem. Soc.* **2002**, *124*, 13770–13789.
- (10) Karadakov, P. B. Aromaticity and Antiaromaticity in the Low-Lying Electronic States of Cyclooctatetraene. *J. Phys. Chem. A* **2008**, *112*, 12707–12713.
- (11) Luz, Z.; Meiboom, S. Structure and Bond Shift Kinetics of Cyclooctatetraene Studied by NMR in Nematic Solvents. *J. Chem. Phys.* **1973**, *59*, 1077–1091.
- (12) Anet, F. A. L. The Rate of Bond Change in Cyclooctatetraene. *J. Am. Chem. Soc.* **1962**, *84*, 671–672.
- (13) Traetteberg, M. Molecular Structure of 1, 3, 5, 7-Cyclooctatetraene. *Acta Chem. Scand.* **1966**, *20*, 1724–1726.
- (14) Tkachev, S. N.; Pravica, M.; Kim, E.; Romano, E.; Weck, P. F. High-Pressure Studies of 1, 3, 5, 7-Cyclooctatetraene: Experiment and Theory. *J. Phys. Chem. A* **2008**, *112*, 11501–11507.
- (15) Bastiansen, O.; Hedberg, L.; Hedberg, K. Reinvestigation of the Molecular Structure of 1,3,5,7-Cyclooctatetraene by Electron Diffraction. *J. Chem. Phys.* **1957**, *27*, 1311–1317.
- (16) Baldovi, J. J.; Clemente-Juan, J. M.; Coronado, E.; Gaita-Arino, A. Molecular Anisotropy Analysis of Single-Ion Magnets Using an Effective Electrostatic Model. *Inorg. Chem.* **2014**, *53*, 11323–11327.
- (17) He, M.; Chen, X.; Bodenstein, T.; Nyvang, A.; Schmidt, S. F.; Peng, Y.; Moreno-Pineda, E.; Ruben, M.; Fink, K.; Gamer, M. T.; et al. Enantiopure Benzamidinate/Cyclooctatetraene Complexes of the Rare-Earth Elements: Synthesis, Structure, and Magnetism. *Organometallics* **2018**, *37*, 3708–3717.
- (18) Summerscales, O. T.; Jones, S. C.; Cloke, F. G. N.; Hitchcock, P. B. Anti-Bimetallic Complexes of Divalent Lanthanides with Silylated Pentalene and Cyclooctatetraenyl Bridging Ligands as Molecular Models for Lanthanide-Based Polymers. *Organometallics* **2009**, *28*, 5896–5908.

- (19) Hosoya, N.; Takegami, R.; Suzumura, J.-i.; Yada, K.; Miyajima, K.; Mitsui, M.; Knickelbein, M. B.; Yabushita, S.; Nakajima, A. Formation and Electronic Structures of Organoeuropium Sandwich Nanowires. *J. Phys. Chem. A* **2014**, *118*, 8298–8308.
- (20) Tokmakov, I. V.; Lin, M.-C. Combined Quantum Chemical/RRKM-ME Computational Study of the Phenyl + Ethylene, Vinyl + Benzene, and H + Styrene Reactions. *J. Phys. Chem. A* **2004**, *108*, 9697–9714.
- (21) da Silva, G.; Moore, E. E.; Bozzelli, J. W. Decomposition of Methylbenzyl Radicals in the Pyrolysis and Oxidation of Xylenes. *J. Phys. Chem. A* **2009**, *113*, 10264–10278.
- (22) Pachner, K.; Steglich, M.; Hemberger, P.; Fischer, I. Photodissociation Dynamics of the Ortho-and Para-Xylyl Radicals. *J. Chem. Phys.* **2017**, *147*, 084303.
- (23) Hemberger, P.; Trevitt, A. J.; Gerber, T.; Ross, E.; da Silva, G. Isomer-Specific Product Detection of Gas-Phase Xylyl Radical Rearrangement and Decomposition Using VUV Synchrotron Photoionization. *J. Phys. Chem. A* **2014**, *118*, 3593–3604.
- (24) Levine, R. D. *Molecular Reaction Dynamics*; Cambridge University Press: Cambridge, U.K., 2005.
- (25) Vernon, M. F. *Molecular Beam Scattering*. Ph.D. Thesis, University of California: Berkeley, CA, 1983.
- (26) Weiss, P. S. *The Reaction Dynamics of Electronically Excited Alkali Atoms with Simple Molecules*. Ph.D Thesis, University of California: Berkeley, CA, 1986.
- (27) Yang, Z.; He, C.; Goettl, S.; Kaiser, R. I.; Azyazov, V. N.; Mebel, A. M. Directed Gas-Phase Formation of Aminosilylene ( $\text{HSiNH}_2$ ;  $X^1A'$ ): The Simplest Silicon Analogue of an Amino-carbene, under Single-Collision Conditions. *J. Am. Chem. Soc.* **2021**, *143*, 14227–14234.
- (28) Gu, X.; Guo, Y.; Zhang, F.; Mebel, A. M.; Kaiser, R. I. Reaction dynamics of carbon-bearing radicals in circumstellar envelopes of carbon stars. *Faraday Discuss.* **2006**, *133*, 245–275.
- (29) Miller, W. B.; Safron, S.; Herschbach, D. Exchange Reactions of Alkali Atoms with Alkali Halides: A Collision Complex Mechanism. *Discuss. Faraday Soc.* **1967**, *44*, 108–122.
- (30) Zhang, J.; Valeev, E. F. Prediction of Reaction Barriers and Thermochemical Properties with Explicitly Correlated Coupled-Cluster Methods: A Basis Set Assessment. *J. Chem. Theory Comput.* **2012**, *8*, 3175–3186.
- (31) Adler, T. B.; Knizia, G.; Werner, H.-J. A Simple and Efficient CCSD (T)-F12 Approximation. *J. Chem. Phys.* **2007**, *127*, 221106.
- (32) Gibson, C. M.; Havenith, R. W. A.; Fowler, P. W.; Jennessens, L. W. Planar Homotropylium Cation: a Transition State with Reversed Aromaticity. *J. Org. Chem.* **2015**, *80*, 1395–1401.
- (33) Barzaghi, M.; Gatti, C. Homoaromaticity Versus Mobius Aromaticity. *J. Chim. Phys.* **1987**, *84*, 783–789.
- (34) Stanger, A. What is... Aromaticity: a Critique of the Concept of Aromaticity—Can it Really be Defined? *Chem. Commun.* **2009**, 1939–1947.
- (35) Jorner, K.; Jahn, B. O.; Bultinck, P.; Ottosson, H. Triplet State Homoaromaticity: Concept, Computational Validation and Experimental Relevance. *Chem. Sci.* **2018**, *9*, 3165–3176.
- (36) Wu, J. I.; Fernández, I.; Mo, Y.; Schleyer, P. v. R. Why Cyclooctatetraene is Highly Stabilized: The Importance of “Two-Way”(Double) Hyperconjugation. *J. Chem. Theory Comput.* **2012**, *8*, 1280–1287.
- (37) Chen, Z.; Wannere, C. S.; Corminboeuf, C.; Puchta, R.; Schleyer, P. v. R. Nucleus-Independent Chemical Shifts (NICS) as an Aromaticity Criterion. *Chem. Rev.* **2005**, *105*, 3842–3888.
- (38) Stanger, A. Nucleus-Independent Chemical Shifts (NICS): Distance Dependence and Revised Criteria for Aromaticity and Antiaromaticity. *J. Org. Chem.* **2006**, *71*, 883–893.
- (39) Jiménez-Halla, J. O. C.; Matito, E.; Robles, J.; Sola, M. Nucleus-Independent Chemical Shift (NICS) Profiles in a Series of Monocyclic Planar Inorganic Compounds. *J. Organomet. Chem.* **2006**, *691*, 4359–4366.
- (40) McIntosh, A. R.; Gee, D.; Wan, J. Electron Spin Resonance Spectra and Indo Calculation of the Cyclooctatrienyl Radical. *Spectrosc. Lett.* **1971**, *4*, 217–225.
- (41) Korth, H. G.; Sustmann, R.; Sicking, W.; Klärner, F. G.; Tashtoush, H. I. Rearrangements of Free Radicals, XIII<sup>[1]</sup>. Thermal and Photochemical Rearrangements of Cyclic  $\text{C}_8\text{H}_9$  Radicals in Adamantane Matrix. *Chem. Ber.* **1993**, *126*, 1917–1927.
- (42) Kaiser, R. I.; Maksyutenko, P.; Ennis, C.; Zhang, F.; Gu, X.; Krishtal, S. P.; Mebel, A. M.; Kostko, O.; Ahmed, M. Untangling the Chemical Evolution of Titan’s Atmosphere and Surface—From Homogeneous to Heterogeneous Chemistry. *Faraday Discuss.* **2010**, *147*, 429–478.
- (43) Yang, Z.; Doddipatla, S.; He, C.; Krasnoukhov, V. S.; Azyazov, V. N.; Mebel, A. M.; Kaiser, R. I. Directed Gas Phase Formation of Silene ( $\text{H}_2\text{SiCH}_2$ ). *Chem. - Eur. J.* **2020**, *26*, 13584–13589.
- (44) Kaiser, R. I.; Gu, X.; Zhang, F.; Maksyutenko, P. Crossed Beam Reactions of Methylidyne [ $\text{CH}(X^2\Pi)$ ] with D2-Acetylene [ $\text{C}_2\text{D}_2(X^1\Sigma_g^+)$ ] and of D1-Methylidyne [ $\text{CD}(X^2\Pi)$ ] with Acetylene [ $\text{C}_2\text{H}_2(X^1\Sigma_g^+)$ ]. *Phys. Chem. Chem. Phys.* **2012**, *14*, 575–588.
- (45) Maksyutenko, P.; Zhang, F.; Gu, X.; Kaiser, R. I. A Crossed Molecular Beam Study on the Reaction of Methylidyne radicals [ $\text{CH}(X^2\Pi)$ ] with Acetylene [ $\text{C}_2\text{H}_2(X^1\Sigma_g^+)$ —Competing  $\text{C}_3\text{H}_2 + \text{H}$  and  $\text{C}_3\text{H} + \text{H}_2$  Channels. *Phys. Chem. Chem. Phys.* **2011**, *13*, 240–252.
- (46) Brink, G. O. Electron Bombardment Molecular Beam Detector. *Rev. Sci. Instrum.* **1966**, *37*, 857–860.
- (47) Daly, N. R. Scintillation Type Mass Spectrometer Ion Detector. *Rev. Sci. Instrum.* **1960**, *31*, 264–267.
- (48) Becke, A. D. A New Mixing of Hartree–Fock and Local Density-Functional Theories. *J. Chem. Phys.* **1993**, *98*, 1372–1377.
- (49) Lee, C.; Yang, W.; Parr, R. G. Development of the Colle-Salvetti Correlation-Energy Formula into a Functional of the Electron Density. *Phys. Rev. B* **1988**, *37*, 785.
- (50) Curtiss, L. A.; Raghavachari, K.; Redfern, P. C.; Rassolov, V.; Pople, J. A. Gaussian-3 (G3) Theory for Molecules Containing First and Second-Row Atoms. *J. Chem. Phys.* **1998**, *109*, 7764–7776.
- (51) Baboul, A. G.; Curtiss, L. A.; Redfern, P. C.; Raghavachari, K. Gaussian-3 Theory Using Density Functional Geometries and Zero-Point Energies. *J. Chem. Phys.* **1999**, *110*, 7650–7657.
- (52) Curtiss, L. A.; Raghavachari, K.; Redfern, P. C.; Baboul, A. G.; Pople, J. A. Gaussian-3 Theory Using Coupled Cluster Energies. *Chem. Phys. Lett.* **1999**, *314*, 101–107.
- (53) Wolinski, K.; Hinton, J. F.; Pulay, P. Efficient Implementation of the Gauge-Independent Atomic Orbital Method for NMR Chemical Shift Calculations. *J. Am. Chem. Soc.* **1990**, *112*, 8251–8260.
- (54) Cheeseman, J. R.; Trucks, G. W.; Keith, T. A.; Frisch, M. J. A Comparison of Models for Calculating Nuclear Magnetic Resonance Shielding Tensors. *J. Chem. Phys.* **1996**, *104*, 5497–5509.
- (55) Frisch, M. J.; Trucks, G. W.; Schlegel, H. B.; Scuseria, G. E.; Robb, M. A.; Cheeseman, J. R.; Scalmani, G.; Barone, V.; Mennucci, B.; Petersson, G. A. et al. *Gaussian 09*, revision D.01; Gaussian Inc.: Wallingford, CT, 2009.
- (56) Werner, H. J.; Knowles, P. J.; Knizia, G.; Manby, F. R.; Schütz, M.; Celani, P.; Korona, T.; Lindh, R.; Mitrushenkov, A.; Rauhut, G. *MOLPRO, version 2010.1, A Package of Ab Initio Programs*; University of Cardiff: Cardiff, UK, 2010.
- (57) Robinson, P. J.; Holbrook, K. A. *Unimolecular Reactions*; Wiley-Interscience: London and New York, 1972.
- (58) Eyring, H.; Lin, S. H.; Lin, S. M. *Basic Chemical Kinetics*; John Wiley & Sons: New York, Chichester, Brisbane, Toronto, 1980.
- (59) Steinfeld, J. I.; Francisco, J. S.; Hase, W. L. *Chemical Kinetics and Dynamics*; Prentice Hall: Upper Saddle River, NJ, 1999.
- (60) Kislov, V. V.; Nguyen, T. L.; Mebel, A. M.; Lin, S. H.; Smith, S. C. Photodissociation of Benzene under Collision-Free Conditions: An Ab Initio/Rice–Ramsperger–Kassel–Marcus Study. *J. Chem. Phys.* **2004**, *120*, 7008–7017.
- (61) He, C.; Zhao, L.; Thomas, A. M.; Morozov, A. N.; Mebel, A. M.; Kaiser, R. I. Elucidating the chemical dynamics of the elementary reactions of the 1-propynyl radical ( $\text{CH}_3\text{CC}$ ;  $X^2A_1$ ) with methyl-

acetylene ( $\text{H}_3\text{CCCH}$ ;  $X^1A_1$ ) and allene ( $\text{H}_2\text{CCCH}_2$ ;  $X^1A_1$ ). *J. Phys. Chem. A* **2019**, *123*, 5446–5462.

## Recommended by ACS

### Electronic States and Nonradiative Decay of Cold Gas-Phase Cinnamic Acid Derivatives Studied by Laser Spectroscopy with a Laser-Ablation Technique

Yuji Iida, Takayuki Ebata, *et al.*

JUNE 17, 2020

THE JOURNAL OF PHYSICAL CHEMISTRY A

READ 

### Mechanistic Insights into Criegee Intermediate–Hydroperoxyl Radical Chemistry

Bai Li, Joseph S. Francisco, *et al.*

AUGUST 03, 2022

JOURNAL OF THE AMERICAN CHEMICAL SOCIETY

READ 

### Large Pressure Effects Caused by Internal Rotation in the *s-cis-syn*-Acrolein Stabilized Criegee Intermediate at Tropospheric Temperature and Pressure

Yu Xia, Donald G. Truhlar, *et al.*

MARCH 09, 2022

JOURNAL OF THE AMERICAN CHEMICAL SOCIETY

READ 

### Hydrogen-Atom-Assisted Uphill Isomerization of *N*-Methylformamide in Darkness

Shih-Yi Tsai, Yuan-Pern Lee, *et al.*

JUNE 30, 2022

JOURNAL OF THE AMERICAN CHEMICAL SOCIETY

READ 

Get More Suggestions >